NANO LETTERS

2007
Vol. 7, No. 7
1923−1928

Carbon Nanotube/Detergent Interactions via Coarse-Grained Molecular Dynamics

E. Jayne Wallace† and Mark S. P. Sansom*

Department of Biochemistry, University of Oxford, South Parks Road, Oxford OX1 3QU, United Kingdom

Received March 14, 2007; Revised Manuscript Received May 10, 2007

ABSTRACT

Detergent interactions with carbon nanotubes are of potential importance in a number of bionanotechnology applications. We investigate the interaction of lysophospholipids with single-walled carbon nanotubes via coarse-grained molecular dynamics. We present compelling evidence that the mechanism of adsorption of these detergents onto a carbon nanotube is dependent upon detergent concentration. Furthermore, the chirality of the carbon nanotube influences the detergent wrapping angle for low detergent concentration. These findings advance our understanding of the mechanism of carbon nanotube solubilization via detergent molecules.

Introduction. Carbon nanotubes (CNTs) possess unique physical and chemical properties leading to a wide array of potential applications.[1] However, an obstacle for the usage of CNTs is their affinity for one another, making it difficult to disperse them as individual tubes in aqueous solution.[2−4] Dissolution of CNTs has been facilitated by covalently attaching polar or charged groups to CNT surfaces. However, this can alter the inherent properties of the tube.[5,6] Thus, attention has turned toward the noncovalent adsorption of lipids and detergents,[7−12] polymers,[13,14] and other biomolecules[15,16] onto the surface of CNTs, thereby preserving the extended π networks of the tubes.

Recent experimental studies have shown that lysophospholipids (single-tailed phospholipids) provide superior solubility for CNTs[7,10,17] compared to the solubility provided by nucleic acids, proteins, and other surfactants. To understand the molecular basis for this superior solubility, and to further enhance the solubility of CNTs, it is important to establish the mechanism of detergent adsorption. Currently there are three common models for adsorption: hemimicelle adsorption of detergent onto CNTs,[9] encapsulation of a CNT within a cylindrical detergent micelle,[13] and random adsorption of detergent onto the tube surface.[12] Transmission electron microscopy images taken in vacuo show that, above their critical micelle concentration (CMC), lysophospholipids form striations spaced by ∼50 Å on the CNT surface,[7,10] implying that adsorption occurs via the hemimicelle model. However, Qiao and Ke[18] have since performed 24 ns atomistic molecular dynamics (MD) simulations of the interaction of zwitterionic lysophosphatidylcholine, or LPC (18-carbon chain), with an (18,0) CNT (length 118 Å and diameter 14 Å) in aqueous solution that opposed the hemimicelle model. Instead, the study found that LPC is predominantly aligned along the CNT axis. At present, it is unclear to what extent the interaction observed in vacuo corresponds to that in aqueous solution. Thus, these experimental and simulation studies highlight the need for further elucidation of the interaction mechanism. Furthermore, atomistic MD simulations of the self-assembly of membrane protein/detergent micelles[19] suggest that a time scale of >20 ns may be needed to allow complete equilibration of a detergent/(bio)molecule micelle. Thus, more extended self-assembly simulation studies of detergent/CNT interactions may provide valuable insights into the mechanism of solubilization of CNTs.

Here we present a computational study of the interaction of LPC with CNTs using coarse-grained (CG) MD. In CG models,[20−24] small groups of atoms are treated as single particles. We utilize the CG methodology developed by Marrink et al.[20] in which approximately four heavy (i.e., not hydrogen) atoms comprise one particle. Particles interact via screened Lennard-Jones and Coulombic potentials, while harmonic terms maintain bond lengths and angles. This model leads to an ∼100 fold increase in speed with respect to atomistic simulations, therefore allowing the capture of CNT/detergent self-assembly processes. The CG methodology developed by Marrink et al.[20] has recently been extended to enable simulation of the self-assembly of proteins and detergent into mixed micelles and of the self-assembly of membrane proteins with lipid bilayers,[25,26] and thus is appropriate to study self-assembly processes of CNT/detergent systems.

We present evidence that the mechanism of LPC adsorption onto a CNT is dependent upon LPC concentration. For

* Corresponding author. E-mail: mark.sansom@bioch.ox.ac.uk. Telephone: +44-1865-275371. Fax: +44-1865-275273.
† E-mail: jayne.wallace@bioch.ox.ac.uk.

10.1021/nl070602h CCC: $37.00
Published on Web 06/09/2007

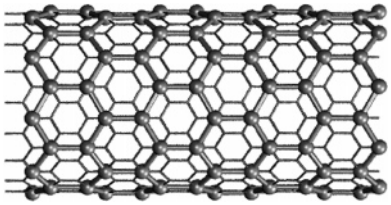

Figure 1. Coarse-grained structure (spheres) of an (18,0) CNT superimposed onto its atomistic structure (thin lines).

low concentrations of detergent, the LPC tails wrap around the CNT, with the wrapping angle between the adsorbed LPC and CNT axis being influenced by the chirality of the CNT. Upon increasing LPC concentration, there is a clear transition to an interaction mechanism in which the LPC molecules have rotated away from the CNT surface so that fewer tail particles are in contact with the CNT. This transition enables more LPC to incorporate into the LPC−CNT complex, thereby reducing exposure of the hydrophobic surface of the CNT and the detergent tails to the aqueous environment, resulting in a more micelle-like assembly.

Methods. CG parameters for LPC were based on those for dipalmitoylphosphatidylcholine (DPPC), as used by Marrink et al.[20] CG parameters for water were also as in Marrink et al.[20] To test the validity of our CG LPC molecules, we performed simulations with ∼250 LPC molecules in a water box. In these simulations, the LPC form ∼7 polydisperse stable micelles (data not shown) with sizes ranging from ∼50 Å to ∼75 Å.

We model CG CNT particles using an approximate 3:1 mapping of the carbon atoms in order to preserve the hexagonal symmetry of the CNT lattice (Figure 1). As a first approximation, we use Marrink's[20] apolar (C) particles to model the CNT particles. However, it should be noted that, in order to examine the robustness of our model, we reduced the CNT−LPC interaction strength relative to the LPC−LPC interaction strength. A significant reduction in CNT−LPC interaction (at least ∼60%) was required before a noticeable change in equilibrium structure was observed (data not shown). CNT particles within ∼10 Å were bonded via a harmonic potential with a force constant of 25 kJ mol^{-1} $Å^{-2}$ in order to maintain the preferred geometry of the nanotube.

All simulations were performed using GROMACS[27,28] at constant temperature (323 K), pressure (1 bar), and number of particles. Simulations were all started with a randomized configuration of LPC molecules. The initial box dimensions were set at 110 × 110 × 110 $Å^3$. Simulation protocols and further information on the CG model are available in the Supporting Information.

Results. To simulate the self-assembly of CNT/detergent complexes, a single finite model CNT was placed in a simulation box containing randomly positioned detergent molecules and water particles. In Figure 2, we show the spontaneous aggregation of a LPC−CNT complex. For repeated (3×) simulations of a CG CNT of length 26 Å and diameter 14 Å, LPC−CNT complexes formed after ∼10 ns. Once formed, the complexes were stable for the length of the simulation (∼200 ns).

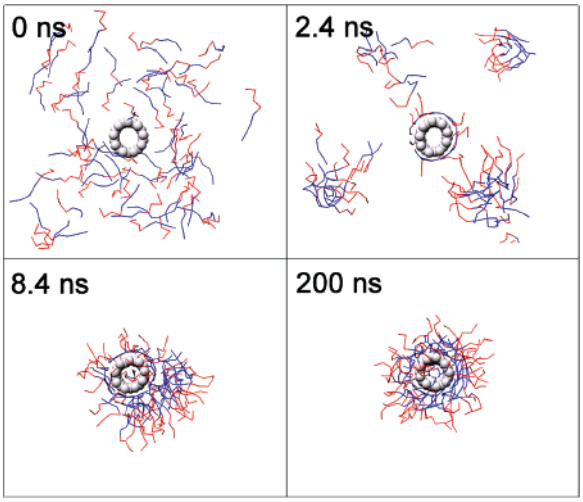

Figure 2. Snapshots of the spontaneous aggregation of 64 LPC molecules with a CG (18,0) CNT. A red line connects the headgroup particles, while a blue line connects the hydrophobic tail particles. Note that the CNT is shown in the same orientation for clarity. However, in the simulations, the CNT is able to move freely.

Note that in experiments the concentration of detergent tends to exceed the critical micelle concentration,[7,10] suggesting that the relevant starting point for simulation is that of preformed detergent micelles. However, detergent solubilization of CNTs requires sonication, leading to a random distribution of detergent molecules. Furthermore, we have performed simulations with preformed LPC micelles. In these simulations, the CNT inserted into the center of a micelle within ∼10 ns (data not shown). This is comparable to the time scale observed in CG simulations of self-assembly of detergent micelles containing simple hydrophobic peptides[25,26] and in the atomistic simulations of Qiao and Ke.[18]

To investigate the nature of the interaction of LPC with CNTs, we calculate the average orientation of LPC molecules with respect to the CNT axis for LPC within the LPC−CNT complex (Figure 3). The average angle θ between LPC molecules and the CNT axis is given by[18]

$$\theta = \arccos\left\langle \frac{|\bar{\nu}_{LPC} \cdot \bar{\nu}_{CNT}|}{|\bar{\nu}_{LPC}||\bar{\nu}_{CNT}|} \right\rangle \quad (1)$$

where $\bar{\nu}_{LPC}$ is the vector from the end LPC tail particle to the center of mass of the headgroup, $\bar{\nu}_{CNT}$ is the CNT axis vector, and $\langle\ \rangle$ represents the statistical average over all LPC molecules in the simulation.

As can be observed in Figure 3, there is a clear correlation between LPC−CNT axis angle and LPC concentration, with the average axis angle increasing upon increasing the detergent concentration. It is unclear from Figure 3 whether or not the detergent tails are wrapped around the CNT, in which case the LPC−CNT axis angle is a wrapping angle (Figure 4a), or alternatively, if the LPC molecules are rotated away from the CNT surface, in which case, the axis angle can be described as a contact angle (Figure 4b).

To clarify the LPC adsorption mechanism, we plot the percentage of contacts between the CNT and the LPC tail

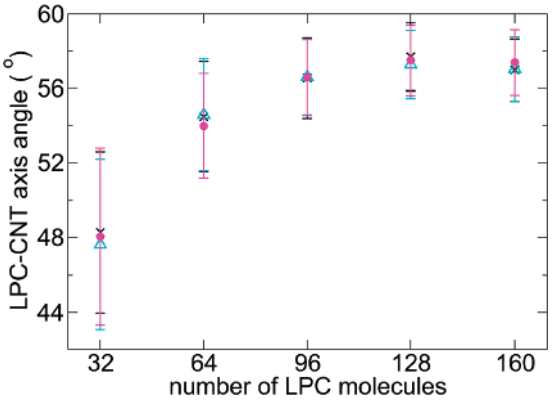

Figure 3. Average LPC−CNT axis angle θ as a function of LPC concentration (θ is as defined in eq 1). Three 400 ns simulations were performed for each concentration of LPC studied, with the axis angles averaged over all LPC molecules during the last 200 ns of each simulation (all LPC were within the LPC−CNT complex in this period). For all simulations, a CG (18,0) CNT of length 26 Å and diameter 14 Å was used.

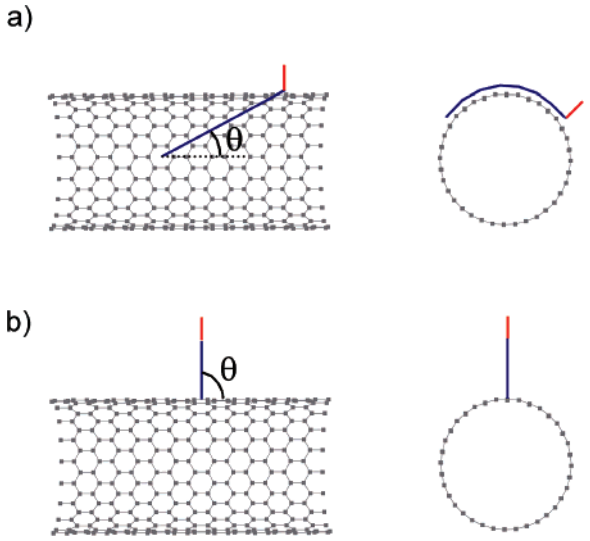

Figure 4. Illustration of an LPC molecule wrapping around a CNT (a), giving rise to a wrapping angle θ with respect to the tube axis. (b) Illustration of an LPC molecule rotated away from the tube surface such that there is a contact angle θ between the LPC and CNT. The same color scheme is used as in Figure 2.

particles (Figure 5). A LPC tail particle is defined to be in contact with the CNT if it is within 6 Å of the CNT.

The percentage of LPC molecules with just one tail particle in contact with the CNT increases upon increasing LPC concentration (Figure 5a). Moreover, for a LPC concentration of 32, ∼60% of LPC have the entire length of their hydrophobic tails in contact with the tube (Figure 5b). This percentage decreases monotonically upon increasing detergent concentration. Hence, there is a clear transition in interaction mechanism upon increasing LPC concentration from surface wrapping to micelle-like. This can be visualized in Figure 6.

In contrast to the atomistic self-assembly simulation study by Qiao and Ke[18]of LPC interacting with (18,0) CNTs, we do not find that LPC align with the CNT axis. Rather, we find that for the CG (18,0) CNT studied, the LPC molecules

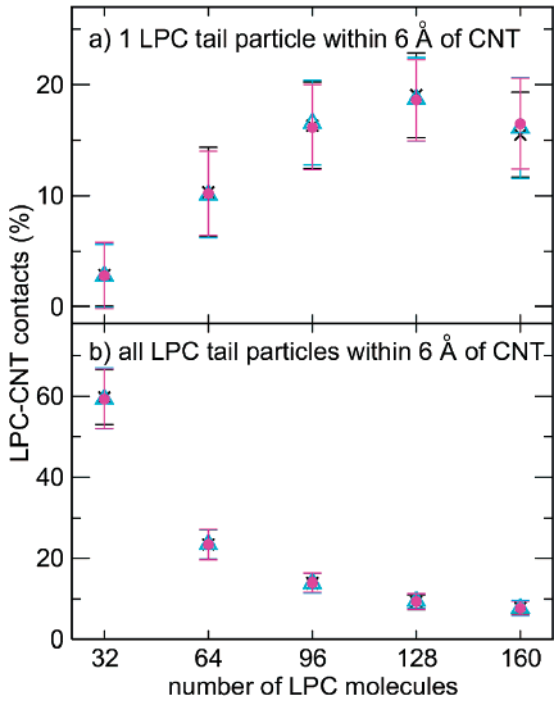

Figure 5. Percentage of LPC molecules that have either one (a) or all four (b) of their tail particles within 6 Å of the CNT. Three 400 ns simulations were performed for each concentration of LPC studied, with the percentage of contacts averaged over the last 200 ns of each simulation. For all simulations, a CG (18,0) CNT of length 26 Å and diameter 14 Å was used.

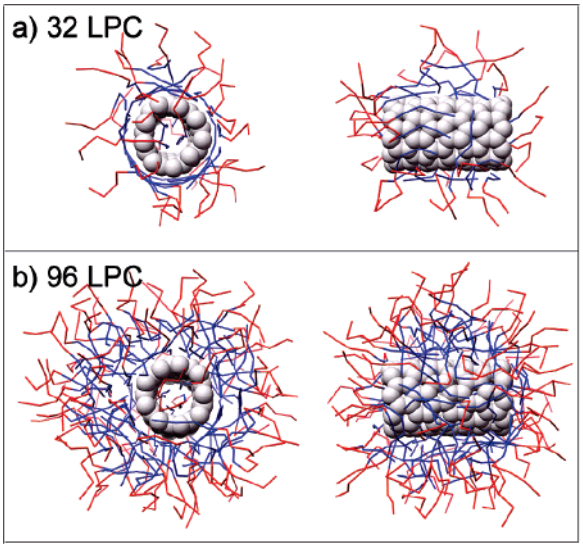

Figure 6. End and side views of equilibrated LPC−CNT complexes with 32 (a) and 96 (b) LPC molecules. The same color scheme is used as in Figure 2.

wrap around the tube for low LPC concentration, with an average wrapping angle ∼48° (Figure 3). For higher detergent concentration, fewer LPC molecules have the whole length of their tails in contact with the CNT (Figures 5b and 6b). Instead, the LPC molecules undergo a rotation such that the contact angle between the tube and LPC is ∼58° (Figure 3). Presumably this transition occurs so that more LPC molecules are able to incorporate into the LPC−CNT complex, thereby minimizing exposure of the hydrophobic

CNT and the LPC tails to the aqueous environment. This interaction mechanism observed at high detergent concentration is more consistent with the "cylindrical detergent encapsulation" model. Note that, at high detergent concentration, we expect the average contact angle between the CNT and LPC to increase as the length of the CNT increases because a smaller percentage of LPC molecules will be bound to the tube ends, i.e., the molecules with a low contact angle.

For 160 LPC molecules, both the percentages of LPC with just one (Figure 5a) and all four (Figure 5b) of their tail particles in contact with the tube are smaller than the respective percentages for 128 LPC molecules. Presumably, this is because the LPC−CNT complex is tightly packed for a detergent concentration of 128 LPC. Hence, any additional LPC molecules are not able to penetrate the complex deeply enough to make contact with the CNT.

Because our results show a clear concentration dependence of the nature of LPC−CNT interactions, it is useful to identify the detergent concentration in our CG study that corresponds with the all-atom simulation study by Qiao and Ke.[18] In the all-atom study, 76 LPC molecules interact with the outer surface of a CNT of length 118 Å and diameter 14 Å. Hence, the average area per LPC is 239 Å^2. To reproduce this area per LPC for our CNT of length 26 Å and diameter 14 Å requires ∼17 LPC molecules. Hence, this low concentration of LPC will be in the surface wrapping regime. It is likely that the discrepancy between our CG study and the atomistic study by Qiao and Ke may reflect the more limited time scale accessible by atomistic simulations. Thus, in the atomistic simulations, the LPC align with the CNT axis after 24 ns, with the detergent headgroups lying adjacent on the tube surface. This conformation of LPC exposes large areas of the hydrophobic LPC tails to the aqueous environment. However, in the CG simulations, the LPC tails wrap around the tube at low detergent concentration, with the detergent headgroups scattered evenly over the complex surface. This conformation of LPC reduces hydrophobic exposure of the LPC tails. It is anticipated that if an all-atom simulation was extended to CG timescales, then the LPC would eventually redistribute over the tube surface so that the hydrophobic exposure of the detergent tails is reduced. It is difficult to estimate the time required for LPC redistribution due to the reduction in diffusivity of the LPC tails in the all-atom representation in comparison to the CG representation. Furthermore, presumably, the conformation of LPC on the CNT in the all-atom study is initially influenced by the first few LPC molecules that interact with the CNT because the time required for a collective change in LPC conformation will be long.

Next we investigate whether or not the interaction between LPC and CNTs is concentration dependent for a CNT of length ∼100 Å. To simulate a long CNT, we fix the tube in the center of a box that has initial dimensions of 90 × 90 × 190 Å^3. We randomly position either 123, 246, or 369 LPC molecules around the CNT and then solvate the box. Figure 7 shows the percentage of contacts between the CNT and the LPC tail particles.

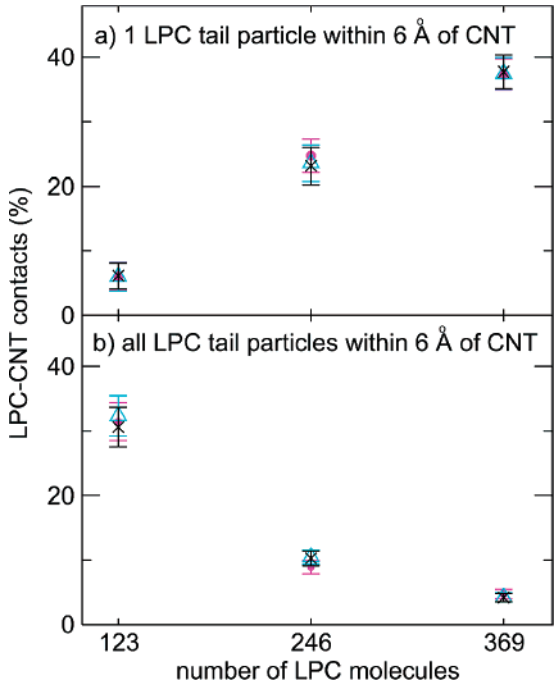

Figure 7. Percentage of LPC molecules that have either one (a) or all four (b) of their tail particles within 6 Å of the CNT. Three 800 ns simulations were performed for each concentration of LPC studied, with the percentage of contacts averaged over the last 200 ns of each simulation. For all simulations, a CG (18,0) CNT of length ∼100 Å and diameter 14 Å was used.

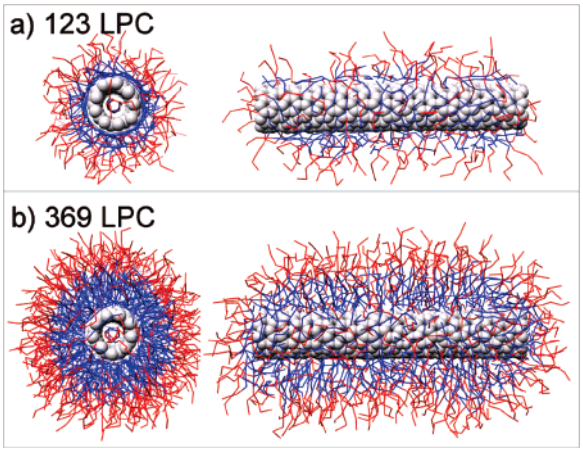

Figure 8. End and side views of equilibrated LPC−CNT complexes with 123 (a) and 369 (b) LPC molecules. The same color scheme is used as in Figure 2.

As shown in Figure 7, a transition in the LPC−CNT interaction occurs upon increasing detergent concentration for a long CNT, consistent with the shorter CNT study (Figure 5). LPC wraps around the CNT at low detergent concentration, while at high detergent concentration, a micelle-like conformation of LPC occurs. This can be observed in Figure 8.

Upon close inspection of the side view of the LPC−CNT complex with 369 LPCs (Figure 8b), a slight curvature can be seen in the overall shape traced out by the detergent molecules. To quantify whether or not the LPC molecules form a striation on the CNT surface, we have calculated the

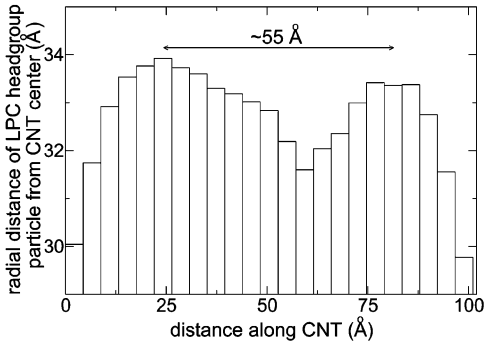

Figure 9. Average radial distance of the terminal LPC headgroup particle from the CNT center as a function of distance along the CNT. The data is averaged over the last 200 ns of an 800 ns simulation of 369 LPC molecules interacting with a CNT of length ~100 Å and diameter 14 Å.

average radial distance of the terminal LPC headgroup particle from the CNT center at set distances along the CNT (Figure 9). Each average was calculated over the last 200 ns of an 800 ns simulation of 369 LPC molecules interacting with a CNT.

As can be observed in Figure 9, a clear LPC striation occurs when a high concentration of detergent interacts with a long CNT. Interestingly, the distance between peaks in the LPC profile is ~55 Å, comparable with the spacing of LPC striations observed via TEM experiments.[7,10] Our results suggest that a hemimicelle model for adsorption may be preferred for a high detergent concentration.

Note that as mentioned earlier, simulations performed for pure LPC in a water box resulted in polydisperse micelles (data not shown). This implies that micelles of varying size are energetically stable, explaining why the two "micelles" interacting with the long CNT (Figures 8b and 9) are of a different size.

Lastly, we investigate the effect that CNT chirality has on the nature of LPC−CNT interactions, where chirality describes the way in which a sheet of graphene is wrapped to form a tube. We study the effect of chirality because, upon close inspection of Figure 6a, it can be observed that the LPC tails are situated within the surface corrugations, or "threadlines", of the tube. Threadlines of a CNT are two aligned but shifted carbon atom chains that are located in the circumferential, helical, and/or tube axis directions depending on the tube chirality. Therefore, CNTs of different chirality should give rise to different average LPC−CNT axis angles. We anticipate that the effect of chirality will be observable when the LPC tails are wrapped around the tube surface, i.e., only for low LPC concentrations.

We study two CNTs of different chirality: a CG zigzag tube based on an atomistic (32,0) CNT and a CG armchair tube based on an atomistic (18,18) CNT. The pitch angles of threadlines in zigzag CNTs are ± 30° and 90° (circumferential) with respect to the tube axis, while the threadlines in armchair CNTs are arranged with pitch angles of 0° and ± 60° with respect to the tube axis. Figure 10 illustrates the location and direction of threadlines for a zigzag and an armchair CNT. Note that the lattice symmetries of the

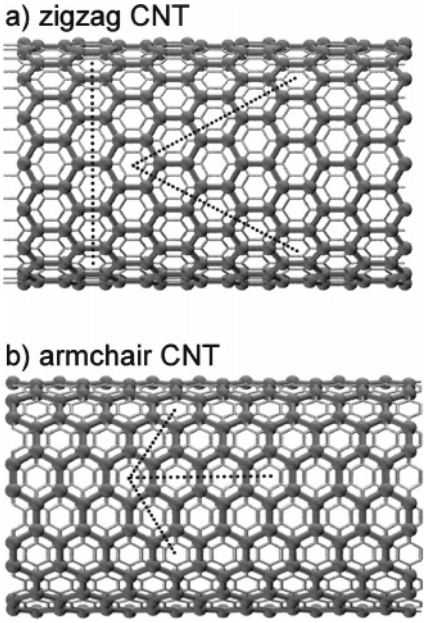

Figure 10. Coarse-grained structure (spheres) of a zigzag CNT (a) superimposed onto an atomistic (32,0) CNT (thin lines); (b) shows a CG armchair CNT superimposed onto an atomistic (18,18) CNT. The dashed lines indicate the direction of the threadlines.

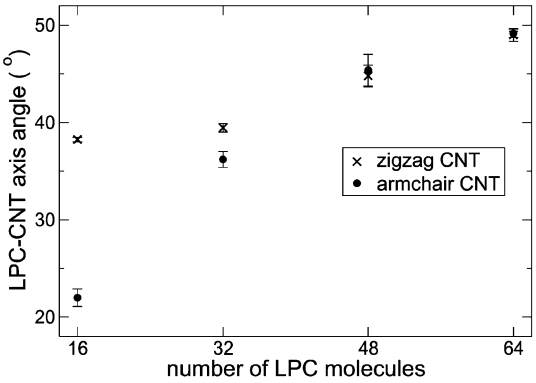

Figure 11. Average LPC−CNT axis angle θ as a function of LPC concentration for a zigzag and an armchair CG CNT. θ is as defined in eq 1. Each axis angle represents an average over all LPC molecules during the last 200 ns of three 400 ns simulations.

underlying atomistic CNT and the respective CG model of a CNT are identical, i.e., the pitch angles of the threadlines are equal.

Both of the tubes we study have a length of ~40 Å and diameter ~25 Å. Hence, any difference in average LPC−CNT axis angle between the two tubes will be due to chirality only. The average orientation of LPC molecules with respect to the CNT axis is shown in Figure 11.

As can be observed in Figure 11, the detergent wrapping angle for an armchair CNT is clearly smaller than the wrapping angle for a zigzag CNT at low LPC concentration. For very low detergent concentration, the LPC molecules coalesce into several domains on the tube surface (Figure 6a illustrates domain formation for a smaller radius tube). LPC tail particles within the domains are situated in the surface corrugations of the tube in order to minimize the van der Waals interaction energy between the tube and LPC.

For an armchair CNT, the average wrapping angle is tending toward 0° (Figure 11), the minimum pitch angle threadline for a tube of this chirality. However, the wrapping angle of LPC on a zigzag CNT is tending toward 30°, the minimum pitch angle threadline for a tube of this chirality (negative wrapping angles are not distinguished in the calculation of Figure 11). Hence, the energetic penalty for coiling the LPC tails is minimized in accordance with the CNT chirality.

Upon increasing LPC concentration, the number of domains on the tube surface increases. Therefore, there will be greater interaction between domains leading to more randomized tail packing. For LPC molecules that are randomly oriented with respect to the CNT axis, the LPC−CNT axis angle $\theta_{\text{random}} = \int_0^{\pi/2} \theta \sin \theta \, d\theta = 1.0 = 57.3°$, hence explaining the trend toward larger axis angles for both tubes studied upon increasing LPC concentration.

For high concentration of detergent, there is little tube surface area available per LPC molecule, inducing the transition from tail wrapping to fewer tail particles being in contact with the tube. Therefore, the lattice structure of the CNT is no longer influencing the conformation of LPC tails leading to $\theta_{\text{armchair}} = \theta_{\text{zigzag}}$, as seen in Figure 11.

Our finding that LPC tails have a smaller wrapping angle around an armchair CNT compared to a zigzag CNT for low LPC concentration complements a previous MD investigation by Wei[29] on the conformation of adsorbed polyethylene molecules (with 100 CH_2 units) on CNTs. In this study, Wei also found that a reduction in tube radius led to a reduction in large-angle polymer wrapping due to the energetic cost of polymer coiling. However, we find that, upon reduction of tube radius for a zigzag CNT, the LPC wrapping angles actually increase (compare Figures 3 and 11). We propose that this is due to the reduction in tube surface area available per LPC molecule, leading to more randomized packing and hence the trend toward the larger angle θ_{random}. Furthermore, the energetic cost for detergent tail coiling is not thought to be large in comparison to the coiling energy for polyethylene because the LPC tails are of length ∼9 Å, while polyethylene with 100 CH_2 units has a length ∼126 Å.

In summary, our CG MD simulations have shown that the mechanism of solubilization of CNTs via LPC is concentration-dependent. Low concentration of detergent leads to the LPC tails adsorbing in between the threadlines of the CNT, therefore minimizing contact between water and the hydrophobic CNT and LPC tails. However, upon increasing the concentration of detergent, there is a clear transition in interaction mechanism with the LPC molecules rotating away from the CNT. This transition enables more LPC to incorporate into the LPC−CNT complex, thereby reducing exposure of the hydrophobic surface of the CNT and the LPC tails to the aqueous environment. The findings reported here shed light on the interaction mechanism of LPC with CNTs and may guide future research on the enhancement of CNT solubilization by different species of detergents.

We are currently exploring converting our equilibrated CG LPC−CNT complexes into atomistic representations, thereby allowing further detailed insights into LPC−CNT interactions. A related multiscale approach to modeling has been applied previously to lipid bilayers.[30,31]

Acknowledgment. We thank Oxford Bionanotechnology IRC, BBSRC, and EPSRC for funding. We thank John Ryan and Maurits de Planque for their interest in this work.

Supporting Information Available: Simulation parameters and details of the CG model. This material is available free of charge via the Internet at http://pubs.acs.org.

References

(1) Dresselhaus, M. S.; Dresselhaus, G.; Avouris, P., *Carbon Nanotubes: Synthesis, Structure, Properties, and Applications*; Springer-Verlag: Berlin, 2001.
(2) Zhao, W.; Song, C. H.; Pehrsson, P. E. *J. Am. Chem. Soc.* **2002**, *124*, 12418.
(3) Star, A.; Stoddart, J. F. *Macromolecules* **2002**, *35*, 7516.
(4) Ausman, K. D.; Piner, R.; Lourie, O.; Ruoff, R. S.; Korobov, M. *J. Phys. Chem. B* **2000**, *104*, 8911.
(5) Chen, J.; Hamon, M. A.; Hu, H.; Chen, Y. S.; Rao, A. M.; Eklund, P. C.; Haddon, R. C. *Science* **1998**, *282*, 95.
(6) Bahr, J. L.; Yang, J. P.; Kosynkin, D. V.; Bronikowski, M. J.; Smalley, R. E.; Tour, J. M. *J. Am. Chem. Soc.* **2001**, *123*, 6536.
(7) Wu, Y.; Hudson, J. S.; Lu, Q.; Moore, J. M.; Mount, A. S.; Rao, A. M.; Alexov, E.; Ke, P. C. *J. Phys. Chem. B* **2006**, *110*, 2475.
(8) O'Connell, M. J.; Bachilo, S. M.; Huffman, C. B.; Moore, V. C.; Strano, M. S.; Haroz, E. H.; Rialon, K. L.; Boul, P. J.; Noon, W. H.; Kittrell, C.; Ma, J. P.; Hauge, R. H.; Weisman, R. B.; Smalley, R. E. *Science* **2002**, *297*, 593.
(9) Islam, M. F.; Rojas, E.; Bergey, D. M.; Johnson, A. T.; Yodh, A. G. *Nano Lett.* **2003**, *3*, 269.
(10) Richard, C.; Balavoine, F.; Schultz, P.; Ebbesen, T. W.; Mioskowski, C. *Science* **2003**, *300*, 775.
(11) Moore, V. C.; Strano, M. S.; Haroz, E. H.; Hauge, R. H.; Smalley, R. E.; Schmidt, J.; Talmon, Y. *Nano Lett.* **2003**, *3*, 1379.
(12) Yurekli, K.; Mitchell, C. A.; Krishnamoorti, R. *J. Am. Chem. Soc.* **2004**, *126*, 9902.
(13) O'Connell, M. J.; Boul, P.; Ericson, L. M.; Huffman, C.; Wang, Y. H.; Haroz, E.; Kuper, C.; Tour, J.; Ausman, K. D.; Smalley, R. E. *Chem. Phys. Lett.* **2001**, *342*, 265.
(14) Huang, W. J.; Fernando, S.; Allard, L. F.; Sun, Y. P. *Nano Lett.* **2003**, *3*, 565.
(15) Zheng, M.; Jagota, A.; Semke, E. D.; Diner, B. A.; McLean, R. S.; Lustig, S. R.; Richardson, R. E.; Tassi, N. G. *Nat. Mater.* **2003**, *2*, 338.
(16) Karajanagi, S. S.; Yang, H. C.; Asuri, P.; Sellitto, E.; Dordick, J. S.; Kane, R. S. *Langmuir* **2006**, *22*, 1392.
(17) Ke, P. C. *Phys. Chem. Chem. Phys.* **2007**, *9*, 439.
(18) Qiao, R.; Ke, P. C. *J. Am. Chem. Soc.* **2006**, *128*, 13656.
(19) Bond, P. J.; Cuthbertson, J. M.; Deol, S. S.; Sansom, M. S. P. *J. Am. Chem. Soc.* **2004**, *126*, 15948.
(20) Marrink, S. J.; de Vries, A. H.; Mark, A. E. *J. Phys. Chem. B* **2004**, *108*, 750.
(21) Shelley, J. C.; Shelley, M. Y.; Reeder, R. C.; Bandyopadhyay, S.; Klein, M. L. *J. Phys. Chem. B* **2001**, *105*, 4464.
(22) Smit, B.; Hilbers, P. A. J.; Esselink, K.; Rupert, L. A. M.; Vanos, N. M.; Schlijper, A. G. *Nature* **1990**, *348*, 624.
(23) Tozzini, V. *Curr. Opin. Struct. Biol.* **2005**, *15*, 144.
(24) Whitehead, L.; Edge, C. M.; Essex, J. W. *J. Comput. Chem.* **2001**, *22*, 1622.
(25) Bond, P. J.; Sansom, M. S. P. *J. Am. Chem. Soc.* **2006**, *128*, 2697.
(26) Bond, P. J.; Holyoake, J.; Ivetac, A.; Khalid, S.; Sansom, M. S. P. *J. Struct. Biol.* **2007**, *157*, 593.
(27) Berendsen, H. J. C.; Vanderspoel, D.; Vandrunen, R. *Comput. Phys. Commun.* **1995**, *91*, 43.
(28) Lindahl, E.; Hess, B.; van der Spoel, D. *J. Mol. Model.* **2001**, *7*, 306.
(29) Wei, C. Y. *Nano Lett.* **2006**, *6*, 1627.
(30) Chang, R.; Ayton, G. S.; Voth, G. A. *J. Chem. Phys.* **2005**, *122*.
(31) Lyubartsev, A. P. *Eur. Biophys. J.* **2005**, *35*, 53.

NL070602H